

# ENHANCEMENT OF MASS AND HEAT TRANSFER FOR IMPROVING THERMAL EFFICIENCY AND WATER PRODUCTIVITY OF MEMBRANE DISTILLATION

Dongjian Cheng<sup>1</sup>, Na Li<sup>1,2,\*</sup>, Jianhua Zhang<sup>3</sup>, Zongli Xie<sup>4,\*</sup>

1 Shaanxi Key Laboratory of Energy Chemical Process Intensification, School of Chemical Engineering and Technology, Xi'an Jiaotong University, Xi'an, Shaanxi 710049, P.R China

2 Key Laboratory of Thermo-Fluid Science and Engineering, Ministry of Education, Xi'an, Shaanxi, 710049, P.R China

3 Institute for Sustainability and Innovation, Victoria University, PO Box 14428, Melbourne, VIC 8001, Australia

4 CSIRO Manufacturing, Private bag 10, Clayton South MDC, VIC 3169, Australia

## ABSTRACT

Membrane distillation (MD) utilizes low-grade thermal energy and alternative energy to drive vapor transport through hydrophobic membrane pores for the application of water desalination, aroma compounds recovery, waste water treatment and concentration of thermo-sensitive solutions. In this work, to overcome commonly observed trade-off problems between thermal efficiency, water flux and water productivity, the simulation and optimization of a series of key objective parameters of MD were conducted by proposing a novel modeling approach. The heat and mass transfer across membrane is synchronously enhanced on account of the interaction effects of operational and module configuration variables to achieve a global optimization of MD.

**Keywords:** membrane distillation; heat transfer coefficient; temperature polarization coefficient; permeate flux; thermal efficiency; water productivity.

## 1. INTRODUCTION

Nowadays there is a rapid growth in using membrane technologies for desalination to deal with the problem of potable water shortage all over the world. Membrane distillation (MD) has been widely studied for desalination of salinity waters with theoretically 100% salt rejection [1]. In MD operation, the volatile species in hot feed evaporate at hydrophobic membrane surface and permeate through porous membrane facilitated by a trans-membrane vapor pressure difference across the membrane [2]. MD is usually conducted at a temperature of 40-80°C, which

makes it possible to utilize alternative energy sources, like geothermal, waste heat, and solar energy [3]. The heat and mass transfer (HMT) is interrelated to each other and there are serious trade-off problems between thermal efficiency, water flux and water productivity of MD process which limit its application. The theoretical models still meet some challenges in treating the problems related to the complicated interactions of variables especially related to various internal design of membrane module [4,5]. Efficient and comprehensive model aiming for high thermal efficiency and water productivity is still lack.

In this study, a novel simulation and optimization approach for MD was proposed by integrating empirical models and theoretical heat and mass transfer models. By this method, it becomes possible to predict and optimize a series of objective parameters such as heat transfer coefficients ( $h_f$ ), temperature polarization coefficient (TPC), water flux ( $N$ ), thermal efficiency ( $\eta$ ), and water productivity ( $P_v$ ) under the interaction effects of complicated operational and configuration variables systematically. Based on the investigation, the global evaluation and optimization of MD were conducted. Feed and permeate inlet temperature ( $T_{wf,in}$ , °C and  $T_{wp,in}$ , °C), feed velocity ( $V_f$ , m/min), module length-diameter ratio ( $R_{ld}$ ) and module packing density ( $D$ , %) are taken into account as influencing factors.

## 2. DCMD EXPERIMENT

Polyvinylidene fluoride hollow fiber membrane modules were used in direct contact membrane distillation (DCMD) (Fig. 1). Feed was circulated through the lumen side of the fibers and cold deionized water in

the shell side of membrane module. Feed/permeate inlet temperature was adjusted by a heater and a chiller, respectively, and were recorded using thermocouples with  $\pm 0.1^\circ\text{C}$  accuracy. The pipes and containers were insulated. The weight gain of water permeate flux was recorded by an analytical balance. The salt rejection of the membranes is as high as over 99.9% for all of the DCMD experiments.

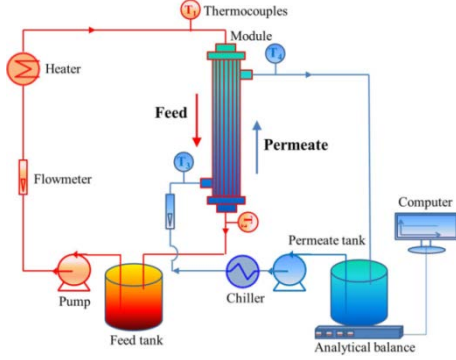


Fig 1 Experimental setup of direct contact membrane distillation.

### 3. HEAT AND MASS TRANSFER MODELING OF DCMD

#### 3.1 Theoretical modeling of DCMD

Fig. 2 is a schematic of trans-membrane heat and mass transfer through a hollow fiber. The difference between membrane surface temperatures ( $T_{mf}$  and  $T_{mp}$ ) induces water vapor pressure gradient across membrane that drives the transport of water vapor through the membrane.

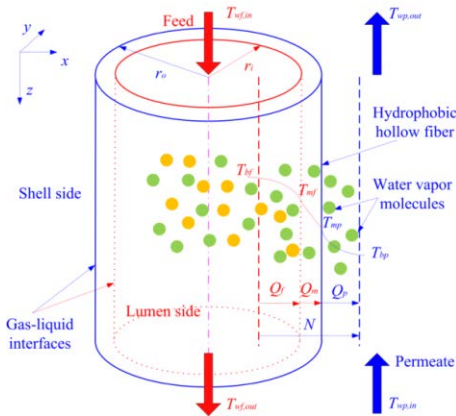


Fig 2 Schematic of heat and mass transport through hollow fiber membrane in DCMD process

Water flux ( $N$ ,  $\text{kg}/(\text{m}^2 \cdot \text{h})$ ) through membrane is dependent on water vapor pressure on feed side and permeate side of membrane ( $P_f$  and  $P_p$ ) as below [6]:

$$N = B_T (P_f - P_p) \quad (1)$$

Here  $B_T$  ( $\text{kg}/(\text{m}^2 \cdot \text{h} \cdot \text{Pa})$ ) denotes mass transfer coefficient across membrane.

The overall mass transport controlled by the Knudsen-Molecular transition region ( $0.01 < K_r < 1$ ) can be expressed as below [6]:

$$B_T = \left( \frac{\tau \delta_m}{1.064 \varepsilon r} \left( \frac{RT}{M_w} \right)^{0.5} + \frac{\tau \delta_m P_a RT}{\varepsilon P D_w M_w} \right)^{-1} \quad (2)$$

Here  $r$ ,  $\varepsilon$ ,  $\tau$  and  $\delta_m$  are the pore radius (m), porosity, pore tortuosity and mean thickness (m) of membrane, respectively.  $R$  is the universal gas constant ( $8.314 \text{ J}/(\text{kg} \cdot \text{K})$ ),  $P_a$  the air pressure (Pa), and  $T_m$  the average temperature across membrane.

The heat transfer in DCMD includes convective transfer on feed/permeate sides of membrane ( $Q_f$  and  $Q_p$ ), the latent heat through membrane pores due to evaporation ( $Q_v$ ), and the conduction heat across the membrane matrix and the medium in membrane pores ( $Q_c$ ) [6].

The temperature polarization coefficient (TPC) is used to evaluate temperature gradient as [6]:

$$TPC = \frac{T_{mf} - T_{mp}}{T_{bf} - T_{bp}} \quad (3)$$

Here  $T_{bf}$  (K) and  $T_{bp}$  (K) are the average temperatures of bulk feed and bulk permeate.

Water productivity per module volume ( $P_v$ ) representing water production capacity of a membrane module is calculated as follows [7,8]:

$$P_v = \frac{\Delta W}{V t} \quad (4)$$

Here  $\Delta W$  (kg) is water mass increment in permeate tank over an operating time  $t$  (h),  $V$  ( $\text{m}^3$ ) is the volume of membrane module.

Thermal efficiency ( $\eta$ ) can be calculated by [6]:

$$\eta = \frac{N \Delta H_v}{N \Delta H_v + \frac{k_m}{\delta_m} (T_{mf} - T_{mp})} \times 100 \quad (5)$$

Here  $\Delta H_v$  (kJ/kg) is the latent heat for water vaporization.

#### 3.2 Simulation and optimization of heat and mass transfer in DCMD

Fig. 3 gives the iterative algorithm of the novel approach by integrating responsive surface methodology (RSM) and theoretical modeling method for simulation and optimization of a series of objective parameters. Firstly, the Nusselt number ( $Nu$ ), feed/permeate side heat transfer coefficients ( $h_f$  and  $h_p$ ), membrane surface temperatures ( $T_{mf}$  and  $T_{mp}$ ), overall mass transfer coefficient ( $B_T$ ), thermal conductivity of porous membrane ( $k_m$ ), permeate flux ( $N$ ), thermal efficiency ( $\eta$ ) and water productivity per

module volume ( $P_v$ ) are calculated successively. Then, these obtained results were used to build a series of RSM models for the objectives as functions of the operational and module configuration variables. Subsequently, the interactions between the influencing variables on the HMT behavior were analyzed based on response surface plots. Then, the optimum conditions for each objective were determined. Finally, the theoretical values of the objectives were obtained by imputing the optimum variables in the theoretical models for comparison.

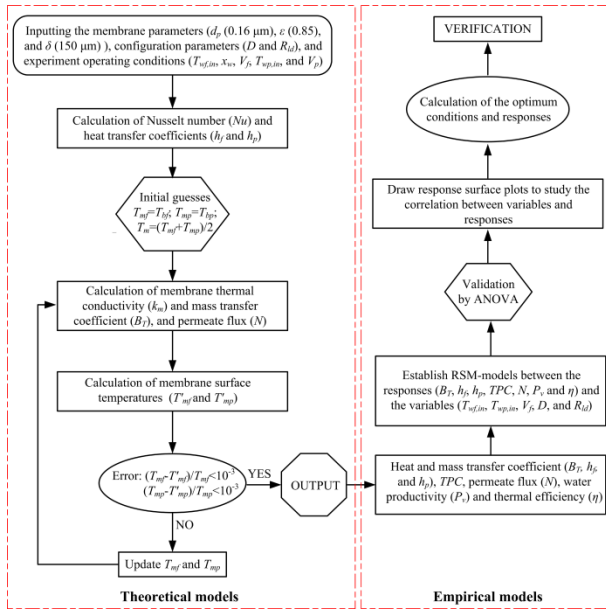


Fig 3 Algorithm for simulation and optimization of heat and mass transfer in DCMd by a RSM-theory coupling method

## 4. RESULTS AND DISCUSSION

### 4.1 Verification and adaptability of theoretical models

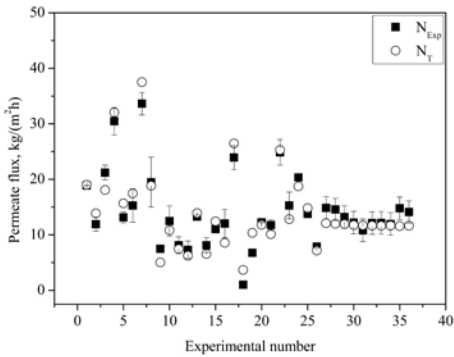


Fig 4 Comparison of simulated water flux ( $N_T$ ) from the Knudsen-molecular diffusion transition model to experimental data ( $N_{EXP}$ )

The DCMd experimental flux were used for verification of the theoretical model. The variables in the experiment are within 40–80°C for  $T_{wf,in}$ , 15–35°C for  $T_{wp,in}$ , 6–54 m/min for  $V_f$ , 5–45% for  $D$ , and 3.3–16.7

for  $R_{ld}$ . The predicted water fluxes ( $N_T$ ) agree well with the simulated ones ( $N_{EXP}$ ) with a relative error of 11.7% (Fig. 4.) The  $K_n$  value of the membrane is 0.6-0.7 which is within 0.01-1 range. The result conforms to the Knudsen-molecular transition mechanism of water vapor transport across the membrane.

### 4.2 Response surface modeling and optimization of objective parameters

Figs. 5-7 show the response surfaces of  $h_f$ , TPC, and  $\eta$ . There is significant interaction effect of feed inlet temperature ( $T_{wf,in}$ ) and module length-diameter ratio ( $R_{ld}$ ) on  $h_f$  (Fig. 5). At various  $T_{wf,in}$  and  $D$ ,  $h_f$  shows a decreasing trend along the flow direction.  $V_f$  and  $R_{ld}$  are the important factors to improve  $h_f$ . High  $h_f$  will be favorable for alleviating temperature polarization and increasing water flux and thermal efficiency.

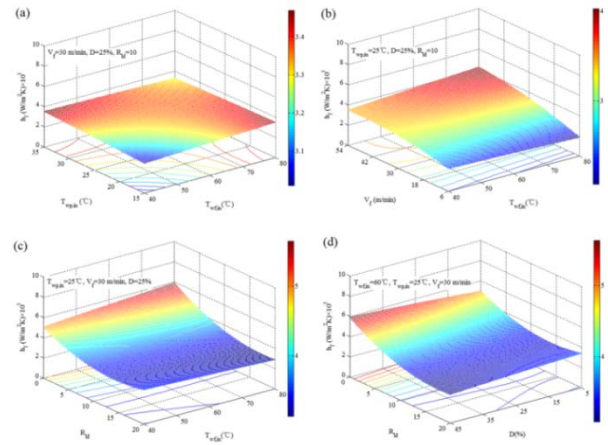


Fig 5 Interaction effects of (a)  $T_{wf,in}$  and  $T_{wp,in}$ ; (b)  $T_{wf,in}$  and  $V_f$ ; (c)  $T_{wf,in}$  and  $R_{ld}$ ; (d)  $D$  and  $R_{ld}$  on feed-side heat transfer coefficient ( $h_f$ ).

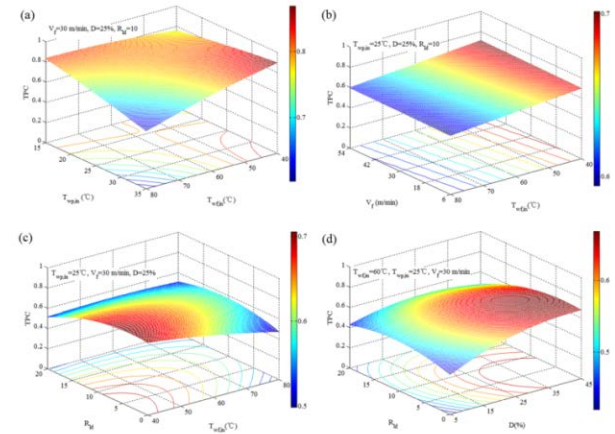


Fig 6 Interaction effects of (a)  $T_{wf,in}$  and  $T_{wp,in}$ ; (b)  $T_{wf,in}$  and  $V_f$ ; (c)  $T_{wf,in}$  and  $R_{ld}$ ; (d)  $D$  and  $R_{ld}$  on temperature polarization coefficient (TPC)

There exist significant coupling effects of the variables on temperature polarization coefficient (TPC) (Fig. 6). The cooperation of high  $T_{wf,in}$  and low  $T_{wp,in}$  as

well as the adoption of low  $R_{ld}$ , high  $D$  and high  $V_f$  is favorable for high  $TPC$  as well as high water flux and thermal efficiency.

$T_{wf,in}$  and  $R_{ld}$  show most strong interaction effect on  $\eta$  (Fig. 7). The negative impact of large  $R_{ld}$  is related to its adverse effect on  $h_f$  as discussed above that increasing  $R_{ld}$  leads to the decline of  $h_f$  along the fiber length (Fig. 5 (c)).

As illustrated above,  $TPC$  and  $h_f$  are greatly affected by the interaction effects of operational and module parameters and their level in turn determines  $N$ ,  $\eta$  and  $P_v$  (Fig. 8). High  $h_f$  with moderate  $TPC$  are beneficial for high  $N$  and  $\eta$ , while high  $h_f$  and  $TPC$  have positive effects on  $P_v$ . The increment in  $P_v$  with  $TPC$  becomes small when  $TPC$  is higher than 0.7. Therefore, high  $h_f$  with moderate  $TPC$  together is capable of leading to the comprehensively high level of MD performance.

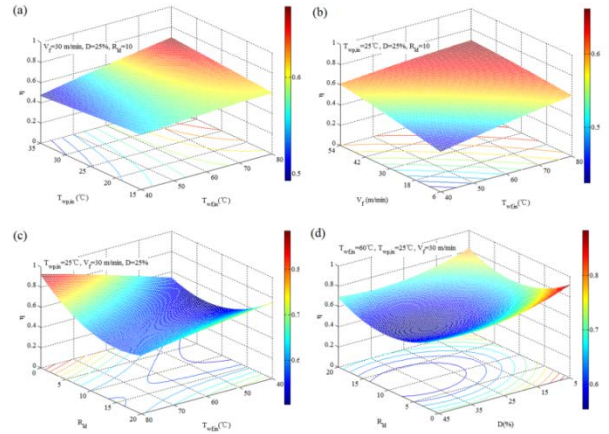


Fig 7 Interaction effects of (a)  $T_{wf,in}$  and  $T_{wp,in}$ ; (b)  $T_{wf,in}$  and  $V_f$ ; (c)  $T_{wf,in}$  and  $R_{ld}$ ; (d)  $D$  and  $R_{ld}$  on thermal efficiency ( $\eta$ )

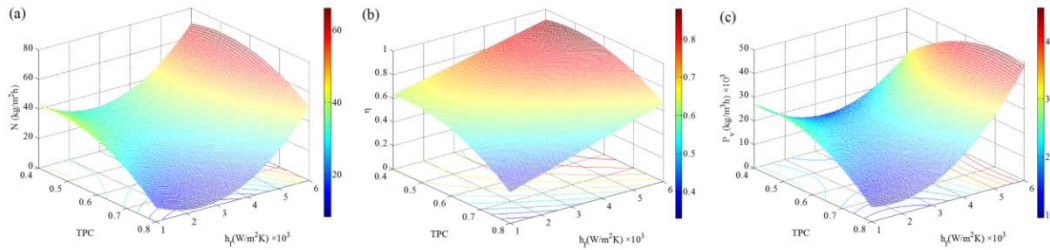


Fig 8 Interaction effect of the temperature polarization coefficient ( $TPC$ ) and heat transfer coefficient ( $h_f$ ) on permeate flux ( $N$ ), thermal efficiency ( $\eta$ ), and water productivity ( $P_v$ )

The optimum conditions for  $P_v$  as well as  $N$  and  $\eta$  were determined. Those for  $P_v$  are shown in Table 1. The predicted results with RSM models are in good agreement with Knudsen-Molecular transition model (K-M model) with 2.1%, 8.5%, 8.3%, 7.1%, and 12.7% of relative errors, respectively.

Table 1 The predicted results of  $h_f$ ,  $h_p$ ,  $TPC$ ,  $N$ ,  $P_v$ , and  $\eta$  as well as the corresponding optimum conditions.

Objective	RSM model	K-M model	Optimum conditions for objectives with *				
			$T_{wf,in}$	$T_{wp,in}$	$V_f$	$D$	$R_{ld}$
$P_v^*$	65684	75208					
$N$	58.49	62.95					
$h_f$	5781	5905	80	15	54	45	3.3
$h_p$	4963	5424					
$TPC$	0.72	0.66					
$\eta$	~1	0.83					

It is found that when  $P_v$  is at highest,  $h_f$ ,  $N$  and  $\eta$  all approach to their own highest level (Fig. 9). The mechanism on the concurrent optimization of the objectives can be easily understood based on their correlation shown in Fig. 8. High  $P_v$  means high overall water productivity of a module at small occupied space and thus low equipment cost which is important for MD commercialization.

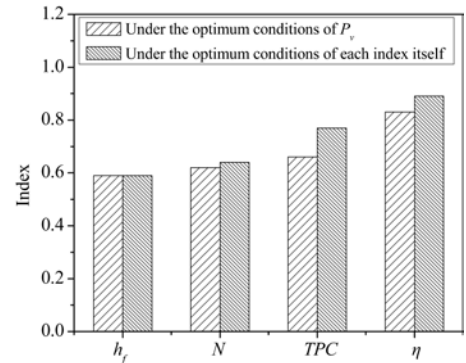


Fig 9 Comparison of the  $h_f$ ,  $N$ ,  $TPC$ , and  $\eta$  under the optimum conditions of  $P_v$  and each index itself

## 5. Conclusions

The conventional modeling by Dusty gas model and Nusselt equation were integrated with response surface methodology to simulate and optimize heat and mass transfer of hollow fiber membranes in DCMD for desalination. Heat transfer coefficient was extremely elevated based on the interaction effects of variables, leading to a simultaneously improvement of high water flux and thermal efficiency. With water productivity ( $P_v$ ) as optimization objective, a global optimization of DCMD performance is realized.

## ACKNOWLEDGEMENT

This work was supported by the National Natural Science Foundation of China [Grant Numbers 21676210].

## References

- [1] Khalifa A, Ahmad H, Antar M, Laoui T, Khayet M. Experimental and theoretical investigations on water desalination using direct contact membrane distillation. *Desalination* 2017;404:22–34.
- [2] González D, Amigo J, Suárez F. Membrane distillation: Perspectives for sustainable and improved desalination. *Renew Sustain Energy Rev* 2017;80:238–59.
- [3] Deshmukh A, Boo C, Karanikola V, Lin S, Straub AP, Tong T, et al. Membrane distillation at water -energy nexus: limits, opportunities, and challenges. *Energy Environ Sci* 2018;11:1177–96.
- [4] Gil JD, Ruiz-aguirre A, Roca L, Zaragoza G, Berenguel M. Prediction models to analyse the performance of a commercial-scale membrane distillation unit for desalting brines from RO plants. *Desalination* 2018;445:15–28.
- [5] Cheng LH, Wu PC, Chen J. Modeling and optimization of hollow fiber DCMD module for desalination. *J Memb Sci* 2008;318:154–66.
- [6] Hitsov I, Maere T, De Sitter K, Dotremont C, Nopens I. Modelling approaches in membrane distillation: A critical review. *Sep Purif Technol* 2015;142:48–64.
- [7] Cheng D, Li N, Zhang J. Modeling and multi-objective optimization of vacuum membrane distillation for enhancement of water productivity and thermal efficiency in desalination. *Chem Eng Res Des* 2018;132:697–713.
- [8] Cheng D, Gong W, Li N. Response surface modeling and optimization of direct contact membrane distillation for water desalination. *Desalination* 2016;394:108–22.